"CONTRIBUTIONS TO THE STUDY OF LASER SCANNERS WITH RISLEY PRISMS FOR OPTICAL COHERENCE TOMOGRAPHY WITH APPLICATIONS IN INDUSTRIAL MEASUREMENTS"

Doctoral Thesis - Abstract

for obtaining the scientific title of doctor at

Polytechnic University of Timisoara

in the doctoral field of *MECHANICAL ENGINEERING*

author *eng. DÎMB ALEXANDRU LUCIAN*

scientific leader Prof. univ. dr. eng. *DUMA VIRGIL-FLORIN*

OCTOBER 2023

Introduction

One-dimensional (1D) and two-dimensional (2D) laser scanners are one of the most utilized optomechatronic modulators. They are employed in a wide range of applications, from commercial (e.g., for barcode scanning) to industrial (from optical metrology to laser manufacturing) and to high-performance systems such as those for biomedical imaging. About forty different configurations of laser scanners have been developed since the early 1970s, but only a few of them are in use today:

(i) Galvanometric (GS) or resonant scanners, the latter being usually built as Micro-Electro-Mechanical Systems (MEMS). Compared to other optical scanners, GS have good characteristics from all points of view: high positioning accuracies and relatively large fields-of-view (FOV), good resolutions, high scanning speeds and reasonable costs, in compact, relatively light constructions. All other scanners have only one or two of these features better than GSs, while the others are weaker. This makes other scanners, such as Risley prisms, more suitable for niche applications, as studied in this thesis;

(ii) Rotational Polygonal Mirrors (PM) can have high rotation speeds (typically up to 54 krpm), therefore also taking into account their number of facets (4-6 for laser printers; up to 128 for high-performance devices); they have much higher scan speeds than GS. However, PMs are larger, more expensive, and affected by mechanical problems due to their high rotational speeds, including vibration, noise, and mechanical wear;

(iii) Refractive - with Risley prisms: their scan speed is also higher than for GSs, but their scan patterns are complicated, non-linear and more difficult to track than the raster scanning produced with two-axis GSs (Fig. 1);

(iv) Holographic, acoustic and electro-optical scanning systems.

Risley prisms [1-16] are utilized in a variety of applications, including interferometry, holography, polarimetry, light attenuation, positioning of aerial targets (e.g. satellites), laser scanning - e.g. in biomedical imaging, for confocal microscopy (CM) or for optical coherence tomography. Risley prisms are an alternative to GSs, PMs, or MEMSs. Sometimes they are also coupled with other scanners, for example a GS, in order to achieve not only 2D but also three-dimensional (3D) scanning.

Laser scanners with Risley prisms consist, in their most common configuration, of a pair of rotating prisms [2-5], but there are also solutions with prisms in oscillating motion or combinations with rotating or oscillating elements (as presented in the part on the state-of-the-art of the thesis). In order to minimize dispersion, a pair of doublets can be utilized, while for

an additional degree of freedom in generating scan patterns, triple prism scanners can be utilized. The diameter of the prisms varies from tens of cm (e.g., for satellite positioning) to sub-millimeter (e.g., for endoscopes).

In order to determine the equations of scan trajectories/*scan patterns*, devices with Risley prisms have been studied analytically in approximate approaches [2], as well as with exact, relatively complex solutions [3,4]. The inverse problem was addressed – in order to obtain the position of the prisms producing an emergent laser beam in a given direction. A fundamental approach was made by Marshall, who proposed in his paper two parameters of these devices for characterizing the scanning trajectories [2]:

– the ratio between the angular speeds: $M = \frac{\omega_2}{\omega_1}$, where: ω_1= the rotation speed of prism 1; ω_2= the rotation speed of prism 2.

– the ratio between the prism angles: $k = \frac{\theta_2}{\theta_1}$, where: θ_1= the angle of prism 1; θ_2 = the angle of prism 2.

Optical Coherence Tomography (OCT) is a non-invasive, high-resolution optical imaging technique that uses the principle of low coherence interferometry to produce images with micrometer-level resolution and millimeter penetration depth [16,17]. While OCT has been originally developed for investigations of the retina, it is now used for a range of biomedical applications, including teeth, skin and endoscopy.

Although OCT was first applied to *in vitro* studies, and it is now used for *in vivo* investigations, as well, as the challenge is to provide real-time images – with video frame capacity. The modern OCT technology has evolved from Time Domain (TD) to Spectral Domain (SD) OCT, which offers higher acquisition speed and better axial resolutions, of up to 2 μm [18] compared to the usual 8-15 μm now (and 30 μm initially). SD-OCT has been developed along two lines of research, either to interrogate the spectrum at the output to the OCT interferometer using a broadband source or a laser source scanned in frequency/Swept Source (SS) and a photodetector. OCT has expanded regarding its area of applications progressively to other fields, such as non-destructive testing (NDT) of materials [19], art conservation applications, and profilometry.

Justification of the choice of the research topic

The motivation of the study has been given by the need to develop faster laser scanning solutions for samples subjected to imaging techniques, such as OCT and confocal microscopy (CM), in order to achieve real-time and eventually *in vivo* imaging of biological samples. It is also necessary to compare the usual scanning mode (raster scanning) in OCT and CM systems with galvanometer scanners (GS) - Fig.1(b), compared to the possibility of (rosette) scanning with Risley prisms - Fig.1(a). Relative to other scanning devices, Risley prisms have specific advantages and disadvantages. Essentially, they provide fast 2D scanning in a more compact build than two-axis GS systems or PM plus GS systems [1]. Also, both their axial size and their diameter can be reduced, making micro-optical solutions possible. While their compactness can only be compared to that of MEMS systems with oscillating mirrors [18], their issues are related to their driving solutions and the complicated laser spot patterns they generate and that must be tracked in order to achieve image reconstruction, for example in CM. Thus, in many studies [2,3] only approximate models (scan patterns) were determined - using the approximation of small angles of the prism (that is, approaching only rotating optical wedges). On the other hand, the exact solutions are relatively complex [4,5].

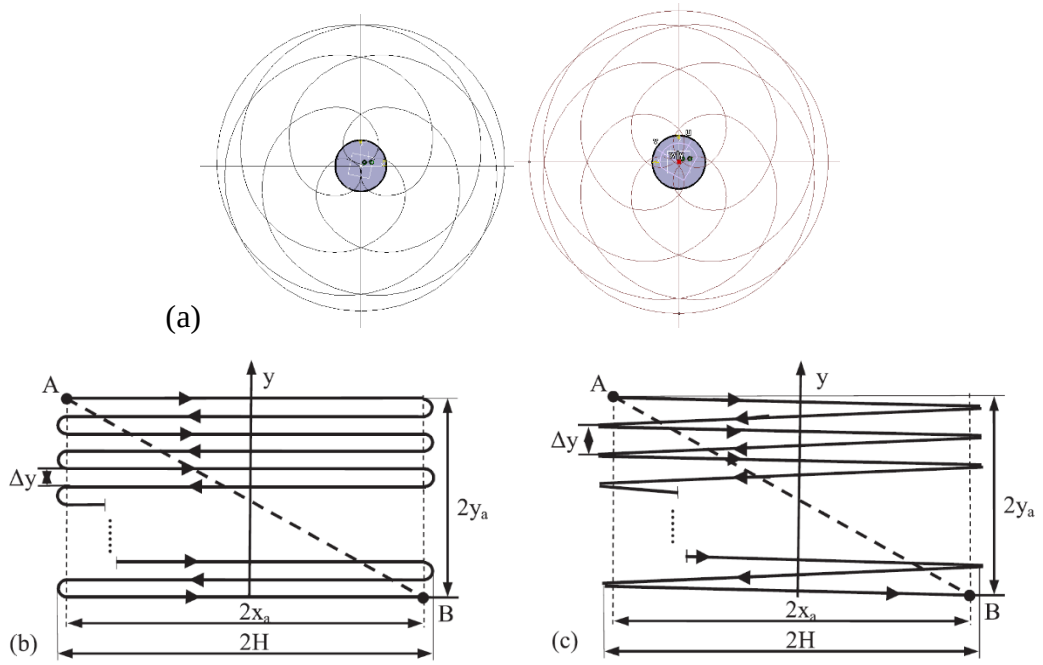

Fig. 1. (a) Scan patterns with Risley prisms; (b,c) galvanometer scanning type 'raster scanning' [20].

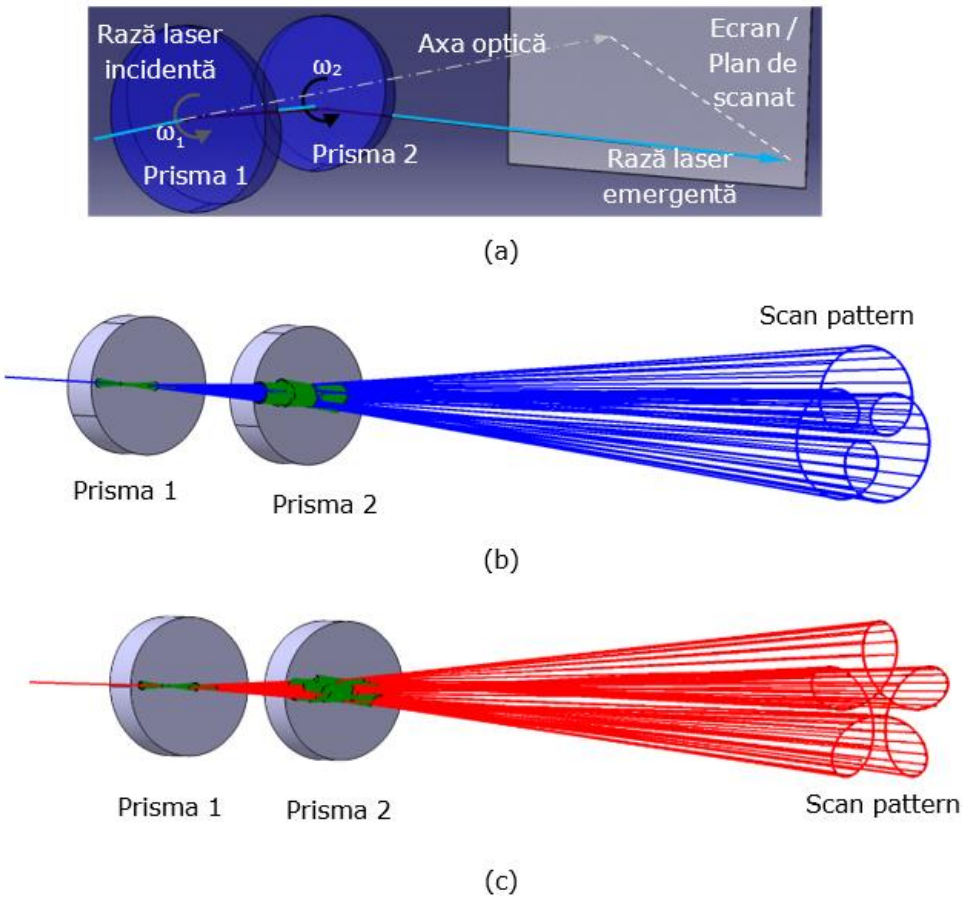

Fig. 2. (a) Pair of rotating Risley prisms, modeled with a commercially available mechanical design program, CATIA V5R20. (b,c) Two light beams generated with CATIA V5R20 to simulate scanning with a pair of rotating Risley prisms. Scan patterns obtained for prisms rotating in the same direction are shown in blue; those obtained for prisms rotating in opposite directions are shown in red [22].

Recently, Risley prisms have been studied by using a new method, not analytical, as in previous studies, but graphical, using a 3D mechanical design program, CATIA V5R20 (Dassault Systèmes, Paris, France) – Fig. 2. **This approach was proposed for the first time by the scientific coordinator, Prof. Duma, in [21].**

The structure of the doctoral thesis

The proposed doctoral thesis comprises a total of eight chapters, divided into two distinct parts. The first two chapters are dedicated to the introduction to the research topic, providing the general context and review of the relevant literature. The next five chapters constitute the main part of the thesis and present the original research, exploring the topic in detail from different perspectives. The last chapter, the eighth, is dedicated to the conclusions, in which the results of the research are summarized and the final conclusions are drawn, offering also perspectives of the research.

Chapter 1 – INTRODUCTION

This chapter presents the field of laser scanners, covering three important aspects: the types of laser scanners available on the market (laser scanner with rotating polygonal head, galvanometer scanners, **refractive scanners – with Risley prism**), the various scanning methods used in this technology (raster, spiral, Lissajous, and **Risley prism scanning**) and a presentation of the applications of these laser scanners in various fields. The entire research study presented in this thesis was carried out with a pair of rotating Risley prisms, using all four configurations that can be obtained depending on the orientation of the two prisms to each other (chapter 3). The method of scanning with these Risley prisms was analyzed. We also used OCT, which is based on laser scanning, to study the roughness of metal surfaces - *chapter 7*.

Chapter 2 - TYPES OF SCANNERS WITH RISLEY PRISMS

In this chapter, a classification of the types of Risley prism scanners has been made, including scanners with pairs of rotating/double prisms, scanners with three rotating prisms, scanners with a pair of oscillating prisms, and combinations of rotating and oscillating prisms. Also, the current state of research in this field is analyzed, highlighting recent developments and discoveries, pointing out the forward and reverse problems associated with Risley scanners.

Chapter 3 - ACCURATE SCAN PATTERNS OF ROTATIONAL RISLEY PRISMS OBTAINED USING THE GRAPHICAL METHOD: A MULTI-PARAMETER ANALYSIS

The chapter presents a series of results published in [V.-F. Duma*, A.L. Dimb, Exact Scan Patterns of Rotational Risley Prisms Obtained with a Graphical Method: Multi-Parameter Analysis and Design, *Applied Sciences* 11, 8451 (**2021**); **IF 2,838**; https://doi.org/10.3390/app11188451] [22].

Chapter 3 presents a study in which we performed a detailed analysis of the scan patterns of a pair of rotating Risley prisms. This analysis involved all the construction parameters of the scanner, besides Marshall's parameters : M (the ratio of angular velocities), k (the ratio between the angles of the prisms), e (the distance between the prisms), L (the length from the system to the scanned plane); but also for the four possible configurations of a laser scanner with a pair

of rotating Risley prisms (Fig.3). In order to simulate these scan patterns, we used an easy-to-use, accurate graphical method, with is exemplified in Fig.4 and 5 [22], which was introduced in previous studies [21]. Through the multi-parametric analysis of the shape and dimensions of the scanning patterns we have identified rules-of-thumb that can be used for the optimal design of optomechanical scanners with Risley prisms, adapted to different application requirements.

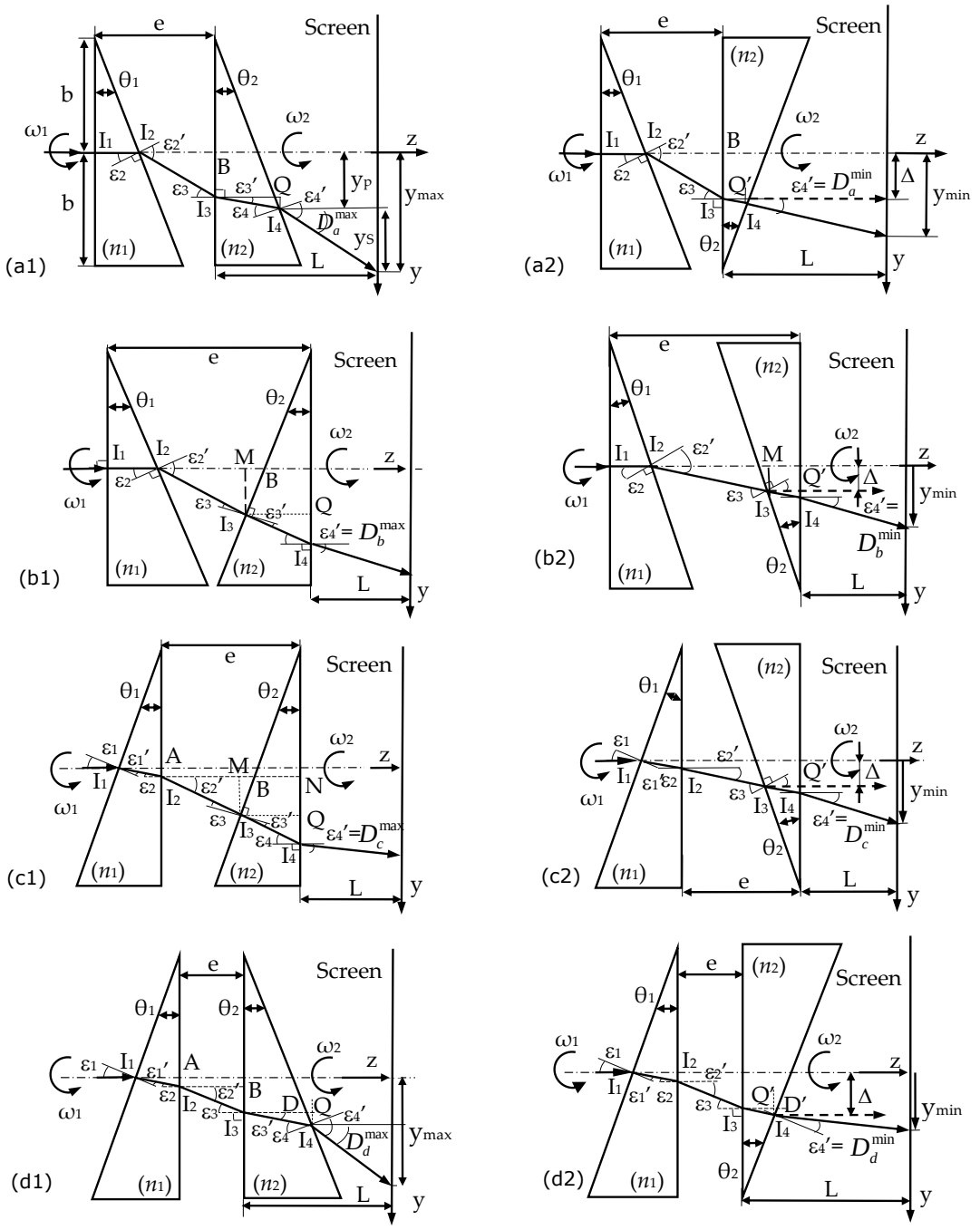

Fig. 3. The four possible configurations of a laser scanner with a pair of rotating Risley prisms: (a) ab-ab; (b) ab-ba; (c) ba-ba; (d) ba-ab. Notations: "a" denotes the diopter perpendicular to the optical axis and "b" the inclined diopter. Each configuration is shown in two extreme characteristic positions of the device, namely with a relative angle of rotation between the two prisms $\varphi = 0$ (column 1) and $\varphi = \pi$ (rad) (column 2) [22].

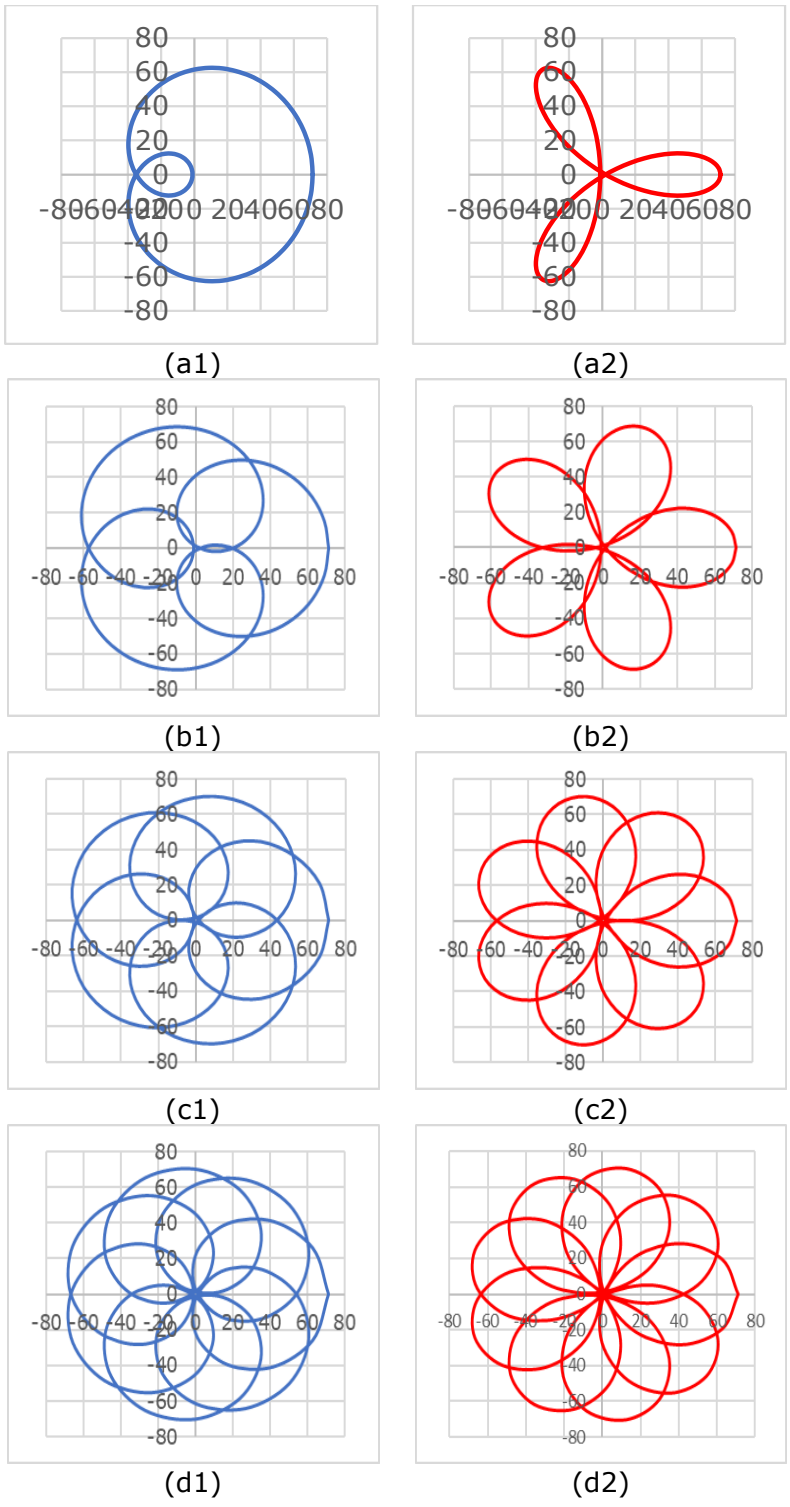

Fig. 4. Study of the scan patterns produced by a pair of rotating Risley prisms (i.e., the ba-ab configuration in Fig.3) for L = 1 m, e = 25 mm and for: (a) |M| = 2; (b) |M| = 4; (c) |M| = 6; (d) |M| = 8. (1) Left column, M > 0; (2) right column, M < 0. The case k = 1 was considered for identical prisms with an individual deviation angle D = (n−1)θ = 2°. The values on the axes are in millimeters [22].

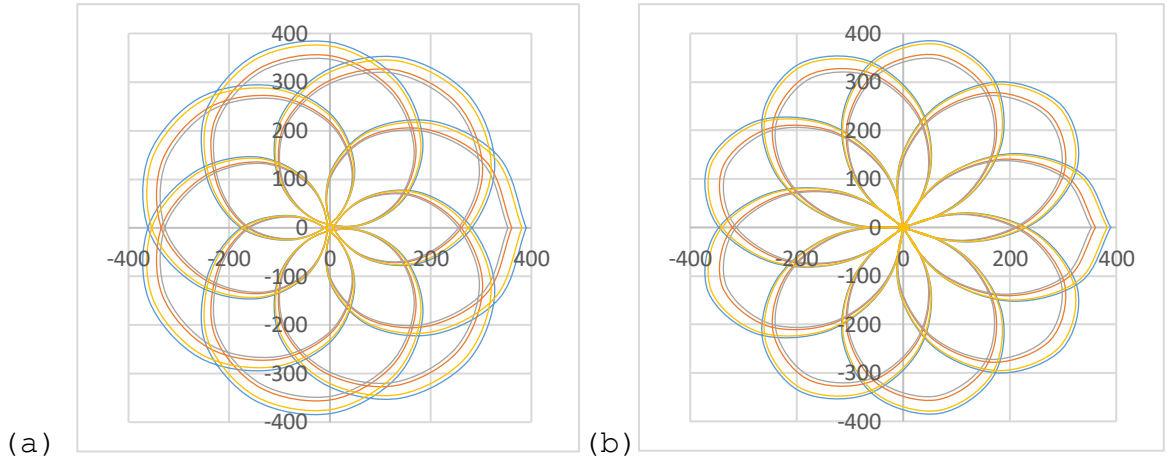

Fig. 5. Comparison between scan patterns of the four scanner configurations shown in figure 3.2, for |M| = 8 and k = 1 (the latter obtained for $D_1 = D_2 = 10°$). (a) Left column, M > 0; (b) right column, M < 0. Values on the axes are in millimeters [22].

Chapter 4 - SYMMETRY OF SCAN PATTERNS OF LASER SCANNERS WITH ROTATIONAL RISLEY PRISMS

This chapter presents a series of results published in [A.L. Dimb, V.-F. Duma*, Symmetries of Scan Patterns of Laser Scanners with Rotational Risley Prisms, *Symmetry-Basel* 15(2), 336 (**2023**); **IF 2.7/2022**; https://doi.org/10.3390/sym15020336] [23]

In this chapter we investigated, in a multi-parametric analysis (using all the characteristics of the device - see the example in Fig.6) the symmetries of the scanning patterns generated by a pair of rotating Risley prisms (example for M = ± 5 in Fig. 7 and 8), which is the most widespread type of laser scanner with such refractive elements. For this analysis we used the graphical method introduced in previous studies [21] and developed in [22], as presented in chapter 3.

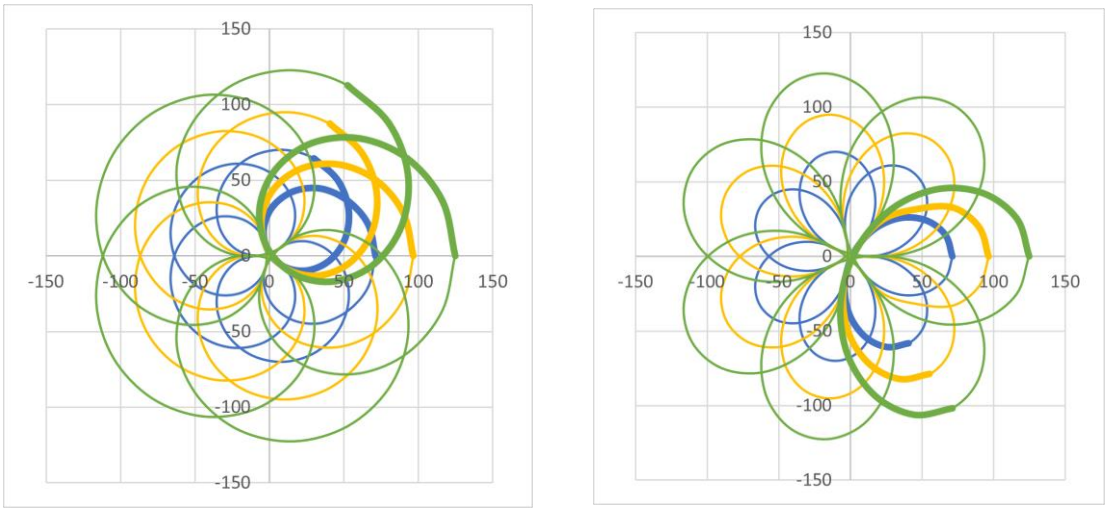

(a) (b)

Fig. 6. Symmetries in the simulated scan patterns for (a) M = 6 and (b) M = −6, for three important increasing successive refractive index (equal) of those two prisms : n = 1.517, n' = 1.7 and n" = 1.9. Scan the corresponding patterns increase successively : blue for n, orange for n' and green for n" [23].

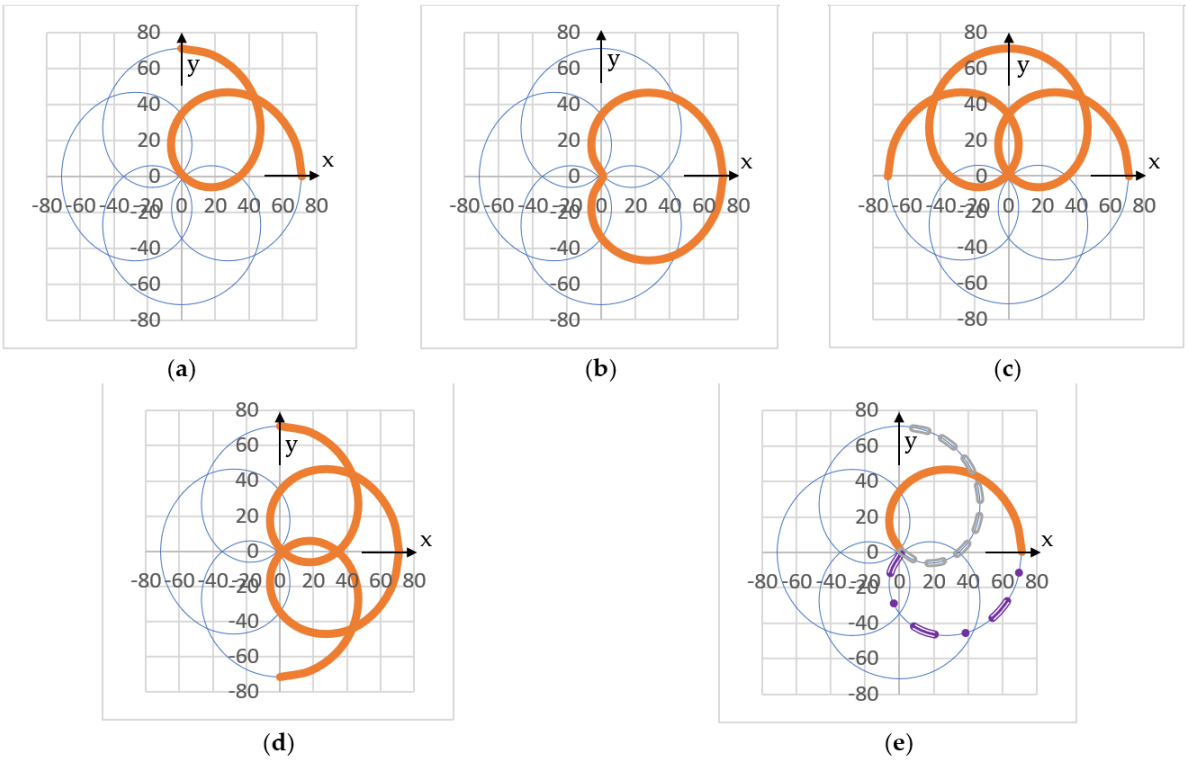

Fig. 7. Symmetries in the simulated scan patterns for M = 5, highlighting the symmetry structures defined in subsection 5, for the relative rotation angles considered: (a) from 0 to π/2; (b) from −π/4 to π/4; (c) from 0 to π; (d) from −π/2 to π/2; (e) from 0 to π/4 [23].

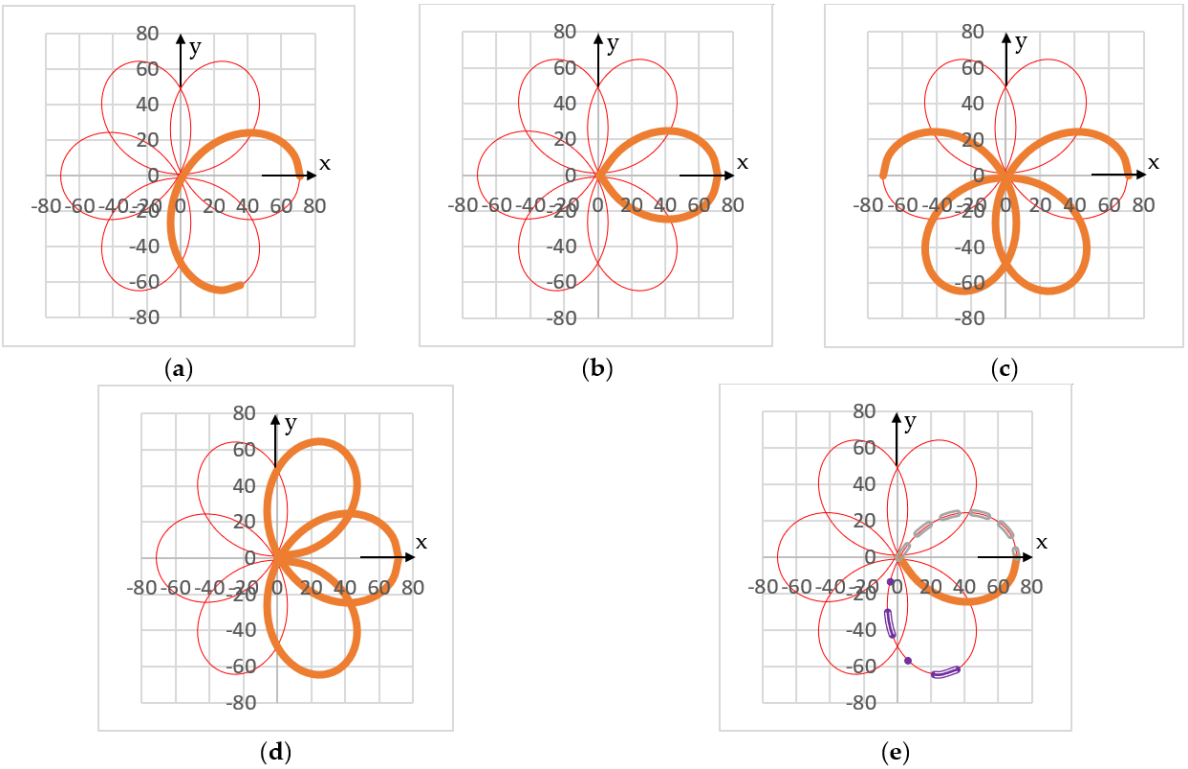

Fig. 8. Symmetries in the simulated scan patterns for M = −2, highlighting the symmetry structures defined in subsection 4.5, for the relative rotation angles considered: (a) from 0 to 2π/3; (b) from −π/3 to π/3; (c) from 0 to π/3 [23].

The results of the simulations highlighted the fact that the parameter *M* (the ratio of the rotation speeds of the prisms) is the determining factor for the symmetries of the scan patterns. Other parameters such as the prism angles (along with their ratio), refractive indices and scanner dimensions (Fig.6) only influenced the dimensions of these scan patterns. We also introduced a new notion, that of "***symmetry structures***", and provided a convenient definition to facilitate the generation of the entire model by replicating a part of it using symmetry. We have illustrated various specific cases and covered a wide range of parameters, including fractional values of *M*, in order to achieve a complete analysis of the subject.

Chapter 5 - SCAN SECONDARY PATTERNS OF A PAIR OF ROTATING RISLEY PRISMS

This chapter discussed various secondary scan patterns (as exemplified in Fig.9) obtained with Risley prisms, using the graphical method developed in the mechanical design program CATIA V5R20.

For this, we created a parameterized system in the program, which was adapted to the chosen configuration, taking into account the basic prism equations and the (minimum possible) number of refractions and internal reflections in the optical system. We analyzed the case of two non-identical rotating Risley prisms, with maximum deflection angles of 2° and 4° (corresponding to k = 0.5, k = 1 and k = 2 for the scanner), for two values of the M parameter, of ±4. For each of these cases, we have presented graphical simulations as well as plots of the x and y coordinates of the point of incidence on the scanned plane. The results presented in this chapter represent an on-going study, which will continue after the completion of this doctoral thesis, being an open direction of research.

Chapter 6 - EXPERIMENTAL STUDY

In order to thoroughly test and study the scan patterns generated by a scanning system with two rotating Risley prisms, we developed and used a dedicated experimental stand (as presented in Fig.10), which this chapter presents. The main objective of this experimental stand was to test and validate experimentally previously formulated theories and hypotheses. Using this stand, we managed to obtain experimental validations for the exactly simulated scan patterns, related to the studies in chapters 3, 4, and 5.

In addition to the theoretical validation, the experimental stand allowed us to analyze the behavior and performance of scanning systems with Risley prisms by comparing simulated scan patterns with those obtained experimentally. The eventual resulting errors were investigated (example - Fig.11 and Table 1), and they are due both to the non-perfect alignment of the components of the experimental stand and to adjustments with limited precision of the parameters that define the system. The experimental stand configured with commercial components from Thorlabs allows the two Risley prisms to be rotated separately with a minimum angular pitch of 2′.

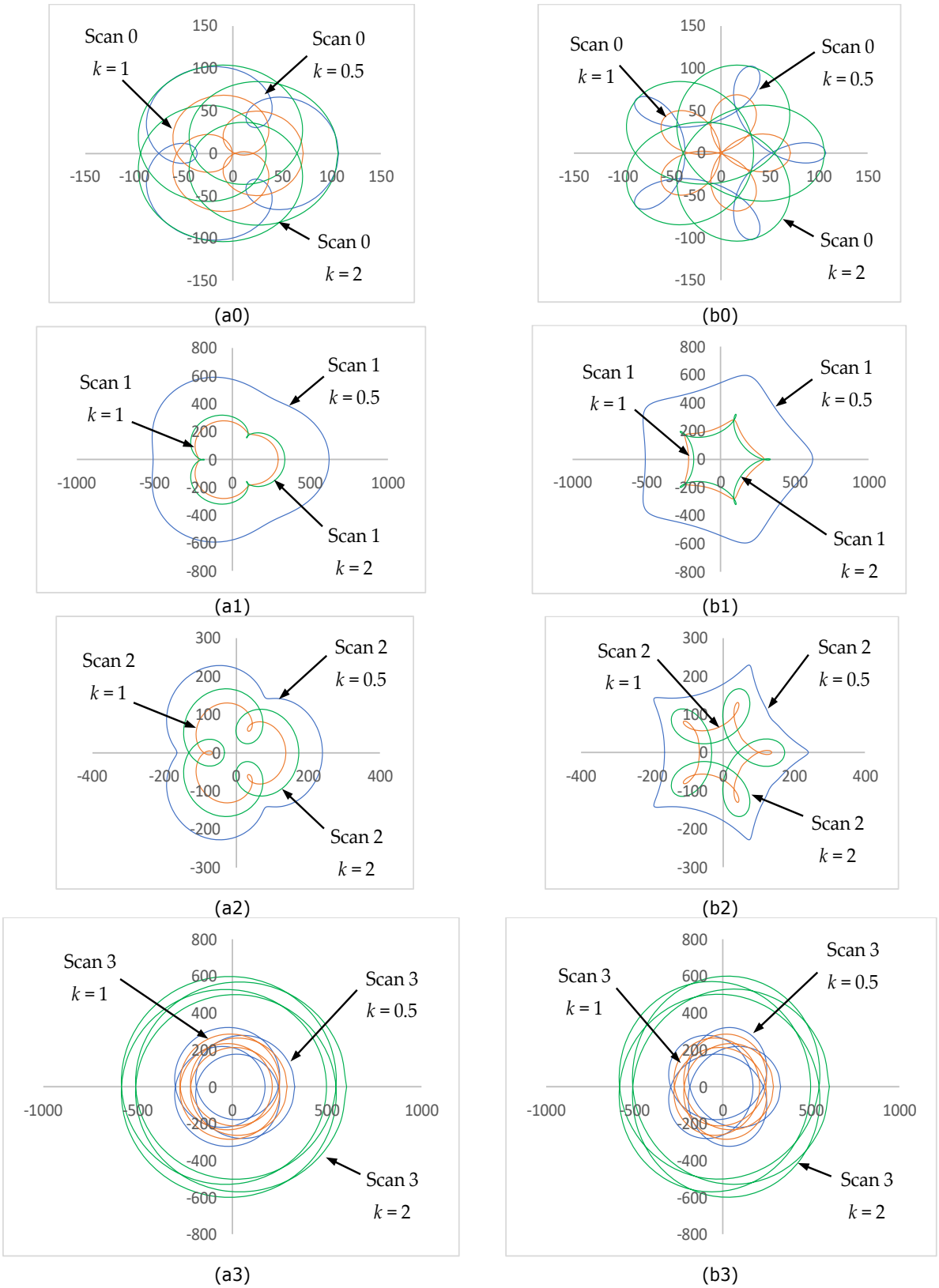

Fig. 9. Scan patterns produced by a pair of Risley prisms in the ab-ab configuration, in a comparison for k = 0.5 (blue), k = 1 (orange) and k = 2 (green), with (a) M = 4 and (b) M = -4: (0) Scan 0 (primary) and secondary, (1) Scan 1, (2), Scan 2, and (3) Scan 3.

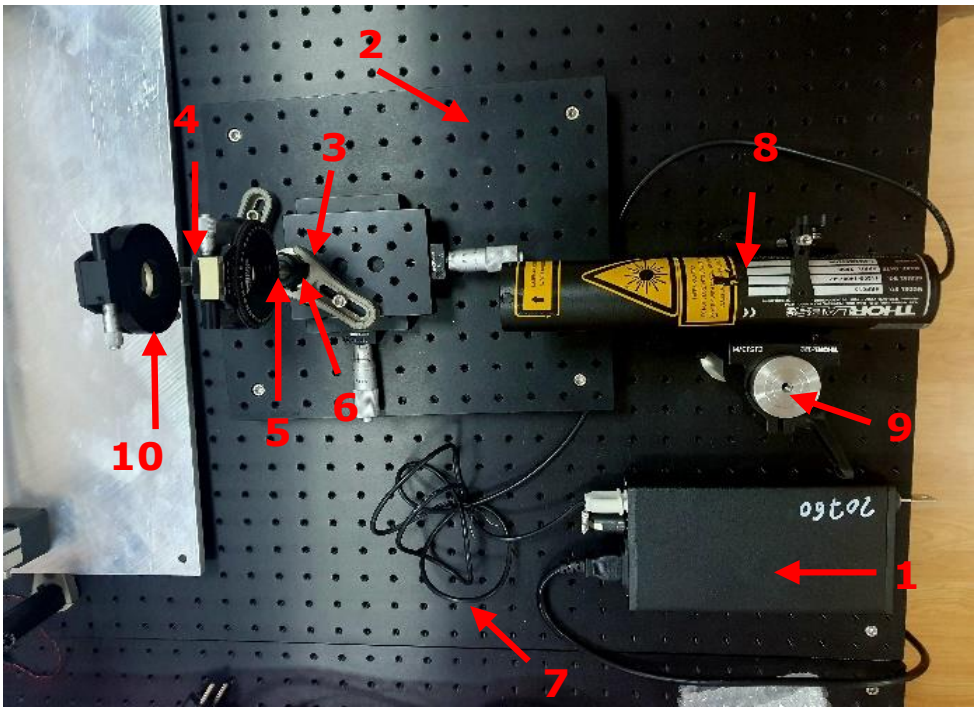

Fig. 10. Presentation showing the components of the experimental stand in the optomechatronics laboratory – for the experimental study of laser scanners with a pair of Risley prisms (in one of 4 possible configurations). Notations: 1. Laser power supply; 2. Support plate; 3. Clamps; 4. Prisma Risley 1 in rotating support; 5,6. Optomechanical parts; 7. Threads; 8. He-Ne laser; 9. Support 2"; 10. Risley prism 1 in rotating stand.

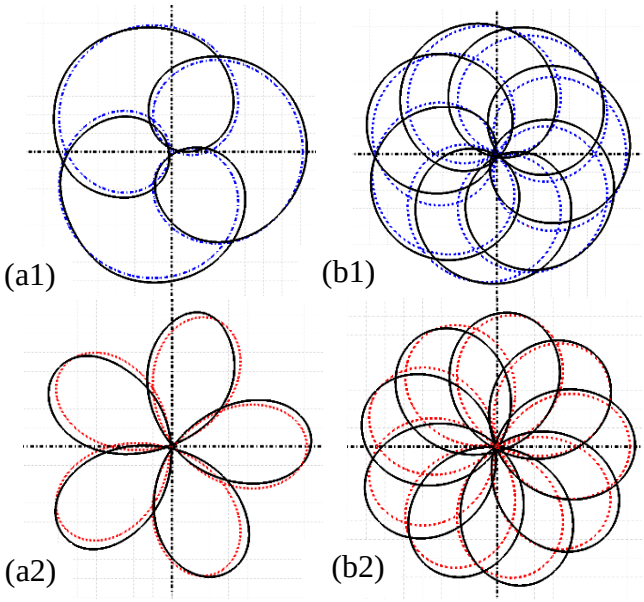

Fig. 11. Scan pattern superimposed (but slightly rotated relative to each other), simulated (in blue for (1) M > 0 and in red for (2) M < 0)) versus experimental (in black), determined for (b) | M| = 2 and (c) |M| = 6 [22].

The ratio of angular speeds	M = 2	M = -2	M = 6	M = -6
The average value of the radius of the field of view: $\overline{R^e} = \frac{1}{\mu}\sum_{j=1}^{\mu} R^e$	70.846	72.692	72.125	72.544
Standard deviation of field of view radius: $\sigma = \sqrt{\frac{1}{\mu}\sum_{j=1}^{\mu}(\overline{R^e} - R^e)^2}$	0.001	0.387	0.536	0.858
Relative error: $\varepsilon^{\%} = (\overline{R^e} - R^e) \cdot 100/\mathrm{R}$	−0.588	2.003	1.206	1.794

Table 1 - Simulated (R) versus experimental (Rm^e) field of view radius of scan patterns - as determined in the investigation shown in Fig.11 [22].

Chapter 7 - APPLICATIONS OF OPTICAL COHERENCE TOMOGRAPHY IN ASSESSING THE ROUGHNESS OF THE SURFACES OF METALLIC MATERIALS

In this chapter we performed roughness measurements on three commercial roughness paths using the optical coherence tomography (OCT) technology (Fig.12), based on point-by-point laser scanning (1000 points for one B-scan / optical section) (Fig. 13a). These commercial tracks have nominal Rz roughness parameter values of 20, 40 and 80 µm, as well as nominal Ra parameter values of 3,6, 9,8 and 18 µm. The main purpose of the research was to determine if the values of the roughness parameters Rz and Ra obtained by means of OCT are compatible with the nominal values of these commercial roughness tracks. The results indicated that as the values of the roughness parameters increased, the differences between the two roughness determination methods became smaller and smaller. In particular, for roughness tracks with nominal values of 40 and 80 µm, the values obtained with OCT were satisfactory compared to the values obtained for the 20 µm track (Table 2).

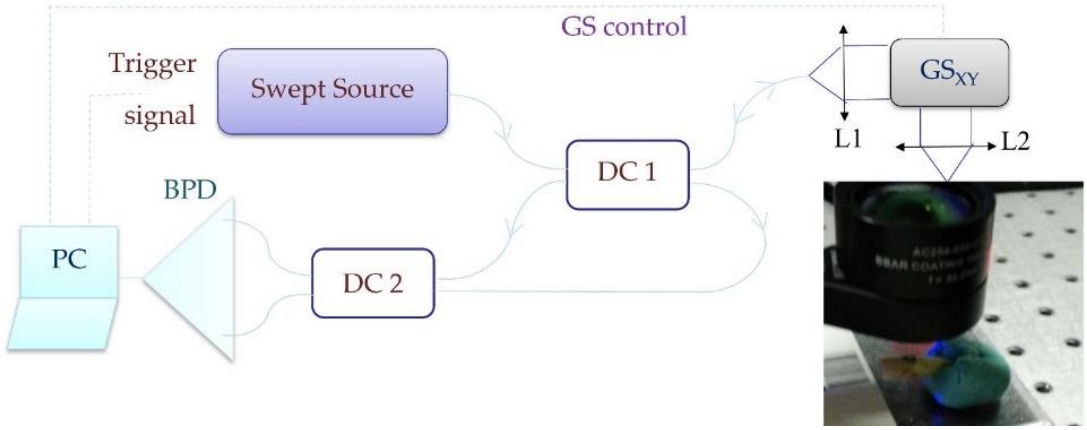

Fig. 12. OCT system with frequency-scanned laser source, Swept Source (SS)-OCT - operation diagram of the experimental system in the laboratory (with galvanometric laser scanner for lateral scanning of the investigated sample).

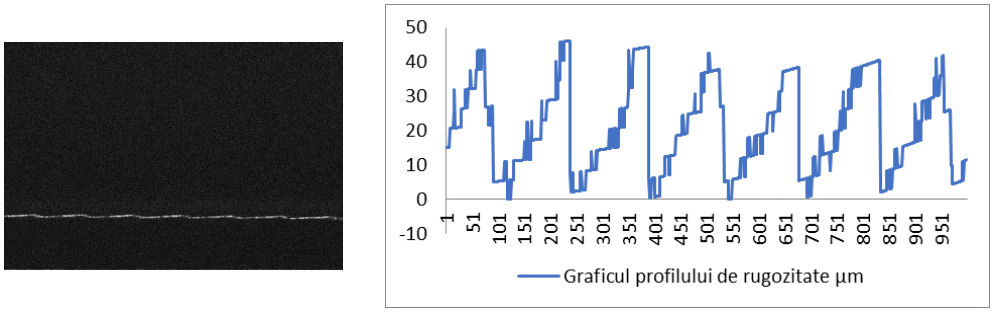

(a) (b)

Fig. 13. (a) B-scan 250.1; (b) Graph of the roughness profile obtained in Excel.

Commercial hold of roughness	Initial Rz (µm)	Rz OCT (µm)	The difference (%)	Initial Ra (µm)	Ra OCT (µm)	The difference (%)
20	20	24.2	21.00	3.6	5.7	58.34
40	40	41.0	2.50	9.8	9.6	- 2.04
80	80	81.5	1.88	18	18.85	4.73

Table 2 - Summary table with roughness parameters for commercial roughness paths of 20, 40, 80.

Chapter 8 – CONCLUSIONS

Risley prisms can be used in a wide range of applications due to their ability to generate precise and controllable scan patterns. Some relevant aspects regarding the importance of these prisms: optical scanning, precision, control and flexibility (they allow the creation of scan patterns with specific characteristics, such as size, shape, symmetry and uniformity), efficiency and speed, diversified applications (laser scanning in remote sensing and cartography, medical imaging systems, optical measurement and inspection, as well as in entertainment and visual arts, etc.).

The research presented in the doctoral thesis ***"CONTRIBUTIONS TO THE STUDY OF LASER SCANNERS WITH RISLEY PRISMS FOR OPTICAL COHERENCE TOMOGRAPHY, WITH APPLICATIONS IN INDUSTRIAL MEASUREMENTS"*** focused on two distinct directions:

I. Study of scan patterns produced with a pair of rotating Risley prisms

A multi-parametric analysis of *the scan patterns* generated by the systems with two rotating Risley prisms was performed [22]. Further on, it was demonstrated that *Marshall's parameter M*, the ratio of the rotation speeds of the two prisms is the determining factor in the symmetry of the scan patterns. The concept of *symmetry structures* was introduced for a more efficient generation of these models [23]. These researches pave the way for the optimal design of Risley prism optomechanical scanners for various applications.

On the other hand, secondary scanning models of the rotating Risley prisms were developed using the mechanical design program CATIA V5R20. These models have brought benefits by increasing the scanning field and the fill factor, having potential applications in biomedical, engineering, but also artistic fields - among others.

II. Optical method of roughness determination

The research included roughness analysis of metal surfaces using optical coherence tomography (OCT), where three commercial roughness paths were used. The measurements results demonstrated that the values of the roughness parameters obtained by OCT are comparable to the nominal values of the roughness paths, with some variations depending on their specific parameters.

This research pave the way for the use of OCT in determining the roughness of metal surfaces, with the potential to offer multiple advantages such as non-contact measurements, speed, efficiency, high resolution, and low long-term costs.

Future research directions

1. Analyses of scan patterns generated with other configurations of Risley prism systems - Fig.14 (with three prisms, respectively with prism doublets - rotating or oscillating) according to the main parameters that define the Risley prism scanning system: M (the ratio angular velocities), k (the ratio between the angles of the prisms), e (the distance between the prisms), L (the length from the system to the scanned plane).
2. Realization of a handheld sample with Risley laser scanners for OCT (Optical Coherence Tomography / Optical Coherence Tomography);
3. Realization of an algorithm for creating OCT images with Risley prisms, as well as its application for different types of metallic (for example in the study of roughness) or non-metallic (including composite materials, plastic, ceramic) samples, but also for biological samples (in collaboration with Victor Babeș University of Medicine and Pharmacy Timișoara).

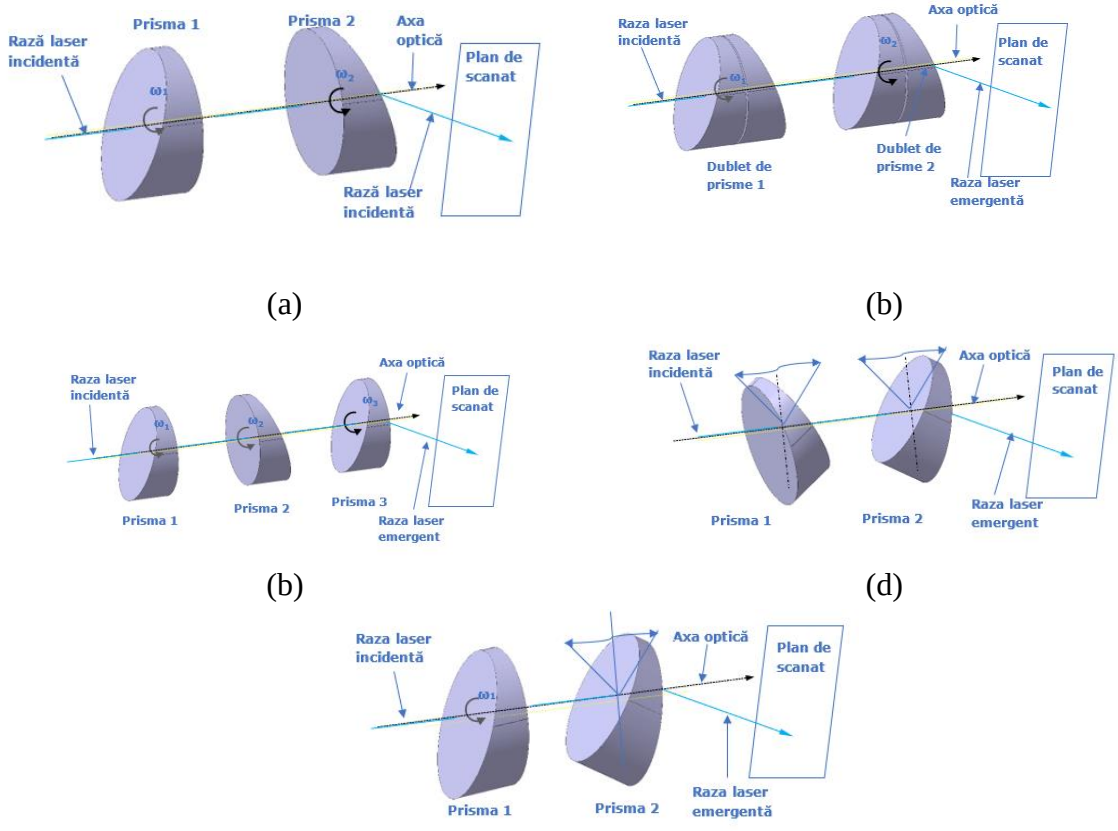

Fig. 14. Types of Risley prism scanners: (a) with a pair of rotating prisms; (b) with a pair of spin doublets; (c) with three rotating prisms; (d) with a pair of oscillating prisms; (e) scanner consisting of a rotating and an oscillating prism – sketches made in the mechanical design program CATIA V5R20 (Dassault Systems, Paris, France).

Bibliography

[1] G.F. MARSHALL, G.E. STUTZ, Eds., Handbook of optical and laser scanning, CRC Press, London, 2011.

[2] G.F. MARSHALL, Risley prisms scan patterns, Proc. SPIE 3787, 74–86, 1999.

[3] Y. LI, Third-order theory of the Risley-prism-based beam steering system, Appl. Opt. 50, 679–686, 2011.

[4] Y. YANG, Analytic solution of free space optical beam steering using Risley prisms, J. Light. Tech. 26, 3576–3583, 2008.

[5] Y. LI, Closed form analytical inverse solutions for Risley-prism-based beam steering systems in different configurations, Appl. Opt. 50, 4302–4309, 2011.

[6] Y. Ge, J. Liu, F. Xue, E. Guan, W. Yan, Y. Zhao, Effect of mechanical error on dual-wedge laser scanning system and error correction, Appl. Opt. 57, 6047-6054 (2018), ISSN 0003-6935.

[7] A. LI, W. Yi, Q. ZUO, W. SUN, Performance characterization of scanning beam steered by tilting double prisms, Opt. Express 24, 23543–23556, 2016.

[8] A. LI, X. LIU, W. SUN, Forward and inverse solutions for three-element Risley prism beam scanners, Opt. Express 25, 7677–7688, 2017.

[9] X. LIU, A. LI, H. CHEN, J. SUN, Z. LU, Scale-adaptive three-dimensional imaging using Risley-prism-based coherent LiDAR, Opt. Letters 48, 2587-2590, 2023.

[10] WANG, J., GE, Y., CHEN, Z.D. et al. Analytic solution for double optical metasurface beam scanners. Sci. Rep. 12, 5912 (2022).

[11] X. LIU, A. LI, An integrated calibration technique for variable-boresight three-dimensional imaging system, Optics and Lasers in Engineering 153, 2022, 107005, ISSN 0143-8166.

[12] X. LIU, A. LI, Multiview three-dimensional imaging using a Risley-prism-based spatially adaptive virtual camera field, Appl. Opt. 61, 3619-3629 (2022). .

[13] SHAN, H.; ZHANG, H.; MA, X.; CAO, K.; JI, C.; TAO, Z.; HAN, J.; WANG, S.; ZHAO, S.; QI, J.; et al. A Fitting Method of Inverting Ozone Concentration Profile Using Ultraviolet Differential Charge-Coupled Device Imaging Lidar. Photonics 2023, 10, 808. .

[14] A. LI, X. LIU, J. SUN, Z. LU, Risley-prism-based multi-beam scanning LiDAR for high-resolution three-dimensional imaging, Optics and Lasers in Engineering 150, 106836, 2022, ISSN 0143-8166.

[15] W. ERB, Rhodonea Curves as Sampling Trajectories for Spectral Interpolation on the Unit Disk. Constr. Approx. (2020).

[16] D. HUANG, E.A. SWANSON, C.P. LIN, J.S. SCHUMAN, W.G. STINSON, W. CHANG, M.R. HEE, T. FLOTTE, K. GREGORY, C.A. PULIAFITO, J.G. FUJIMOTO, Optical coherence tomography, Science 254, 1178-1181, 1991.

[17] W. DREXLER, M. LIU, A. KUMAR, T. KAMALI, A. UNTERHUBER, R.A. LEITGEB, Optical coherence tomography today: speed, contrast, and multimodality, J. Biomed. Opt. 19, 071412, 2014.

[18] A. COGLIATI et al., V.-F. DUMA, J.P. ROLLAND, MEMS-based handheld scanning probe with pre-shaped input signals for distortion-free images in Gabor-Domain Optical Coherence Microscopy, Opt. Express 24, 13365–13374, 2016.

[19] GH. HUTIU, V.-F. DUMA, D. DEMIAN, A. BRADU, A. GH. PODOLEANU, Assessment of ductile, brittle, and fatigue fractures of metals using optical coherence tomography, Metals 8(2), 117, 2018.

[20] V.-F. DUMA, Laser scanners with oscillatory elements: Design and optimization of 1D and 2D scanning functions, Appl Math Modelling 67, 456-476, 2019.

[21] V.-F. DUMA, A. SCHITEA, Laser scanners with rotational Risley prisms: Exact scan patterns, Proceedings of the Romanian Academy, Series A 19(1), 53-60, 2018.

[22] V.-F. DUMA A-L. DIMB, Exact Scan Patterns of Rotational Risley Prisms Obtained with a Graphical Method: Multi-Parameter Analysis and Design, Applied Sciences 11, 8451 (2021);* ***IF 2.838****.*

[23] A.-L. DIMB and V.-F. DUMA, Symmetries of Scan Patterns of Laser Scanners with Rotational Risley Prisms, Symmetry 2023, 15(2), 336;* ***IF 2.7****.*